

Structural plasticity of single chromatin fibers revealed by torsional manipulation

Aurélien Bancaud¹, Natalia Conde e Silva², Maria Barbi³, Gaudeline Wagner¹, Jean-François Allemand⁴, Julien Mozziconacci³, Christophe Lavelle^{2,3}, Vincent Croquette⁴, Jean-Marc Victor³, Ariel Prunell² & Jean-Louis Viovy¹

Magnetic tweezers were used to study the mechanical response under torsion of single nucleosome arrays reconstituted on tandem repeats of 5S positioning sequences. Regular arrays are extremely resilient and can reversibly accommodate a large amount of supercoiling without much change in length. This behavior is quantitatively described by a molecular model of the chromatin three-dimensional architecture. In this model, we assume the existence of a dynamic equilibrium between three conformations of the nucleosome, corresponding to different crossing statuses of the entry/exit DNAs (positive, null or negative, respectively). Torsional strain displaces that equilibrium, leading to an extensive reorganization of the fiber's architecture. The model explains a number of long-standing topological questions regarding DNA in chromatin and may provide the basis to better understand the dynamic binding of chromatin-associated proteins.

The genetic material of eukaryotic cells is organized into chromatin, a nucleoproteic structure whose repetitive unit is the nucleosome¹. The core particle of the nucleosome consists of 147 bp of DNA wrapped 1.65 times around an octamer containing two copies each of the four core histones, H2A, H2B, H3 and H4 (ref. 2). This leads to both compaction and topological deformation of the DNA by one negative turn per nucleosome ($\Delta Lk \sim -1$, Lk being the linking number³). *In vivo*, regularly distributed nucleosome arrays with a repeat length of ~ 200 base pairs¹ fold into 30-nm fibers, whose modulated compaction is thought to be associated with a differential accessibility of DNA⁴ to interactions with various factors, as required for DNA activity. A better knowledge of chromatin organization is thus expected to improve our understanding of the regulation of DNA transactions *in vivo*.

Bona fide nucleosome arrays can be reconstituted *in vitro*, and single-molecule techniques now offer a direct approach to study their molecular dynamics in real time. Force micromanipulation has revealed the existence of an internucleosomal attraction that maintains the higher-order chromatin structure under physiological conditions⁵ and shown a reversible peeling of ~ 80 bp of nucleosomal DNA below 15 pN (ref. 6), presumably associated with the destabilization of H2A–H2B dimers. Above this force, discrete disruption events of 25 nm each, attributed to the dissociation of tetrasomes ((H3–H4)₂–DNA complexes)^{6,7}, have been observed.

In this study, we performed the first torsional nanomanipulation of single chromatin fibers using magnetic tweezers⁸. We observed that nucleosome arrays reconstituted on 5S tandemly repeated positioning

sequences⁹ with core histones purified from chicken erythrocytes can accommodate large amounts of negative or positive supercoiling without much change in their length. We propose a quantitative model based on a dynamic equilibrium between the three conformations of the nucleosome previously identified through the minicircle approach (a single nucleosome reconstituted on a DNA minicircle)¹⁰. In these states, the nucleosome entry/exit DNAs can cross negatively (as in the canonical structure²) or positively, or not cross at all. The model fits the chromatin length-versus-torsion response at various levels of compaction and under stretching forces ranging from 0.09 to 5 pN. It also shows how the torsional constraint can force nucleosomes to switch conformation and can induce a large and reversible reorganization of the fiber architecture. These findings provide simple answers to long-standing topological puzzles about DNA in chromatin. Moreover, the ability of chromatin to undergo fast and reversible structural reorganizations, revealed by this study, may underlie the dynamic nature of the binding of numerous chromatin-associated proteins^{11,12}.

RESULTS

Torsion

Nucleosome arrays were reconstituted by stepwise dilution using a linear DNA containing 36 tandemly repeated 208-bp 5S positioning sequences⁹ and purified core histones. These fibers were then flanked by two naked DNA spacers, to avoid histone-mediated hydrophobic interaction with the surfaces, and by two 'stickers' that link the fiber to

¹Institut Curie, UMR 168, 75231 Paris, France. ²Institut Jacques Monod (UMR 7592), 2 Place Jussieu, 75251 Paris, cedex 05, France. ³Laboratoire de Physique Théorique de la Matière Condensée (UMR 7600), 4 Place Jussieu, 75252 Paris, cedex 05, France. ⁴Laboratoire de Physique Statistique (UMR 8549), 24 Rue Lhomond, 75231 Paris, cedex 05, France. Correspondence should be addressed to J.-L.V. (jean-louis.viovy@curie.fr) or A.P. (prunell@ccr.jussieu.fr).

Received 23 December 2005; accepted 14 March 2006; published online 16 April 2006; doi:10.1038/nsmb1087

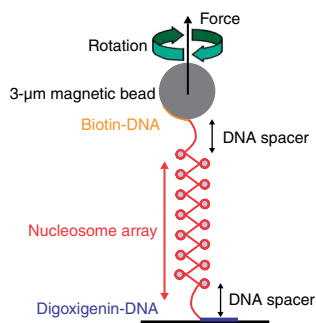


Figure 1 Schematic of the experiment. A single nucleosome array (~ 7.5 kbp), sandwiched between two naked DNA spacers (~ 600 bp each), is linked to a coated surface and to a magnetic bead. A pair of magnets placed above this molecule exerts controlled torsional and extensional constraints⁸.

the coated bottom of the flow cell and to the paramagnetic bead, respectively (Fig. 1, blue and orange segments). A pair of magnets was placed above this construction, and different torsions were applied by rotating the magnets about the vertical axis. The magnets' vertical position specifies the stretching force, that is, the fiber extension, which was measured by recording the three-dimensional position of the bead⁸.

The typical torsional behavior of a single chromatin fiber in low-salt buffer B_0 (see Methods) is shown in Figure 2a at 0.34 pN (blue curve). After chemical dissociation of the nucleosomes, the response of the corresponding naked DNA was obtained (red). This latter curve displays a mechanical effect of torsion and an asymmetry for negative supercoiling. These features are the signatures of an unnicked single-duplex DNA⁸. Compared to naked DNA, chromatin is shorter by ~ 1.35 μm , and its center of rotation is shifted by -24 ± 2 turns. This corresponds to a shortening of ~ 55 nm per negative turn, as expected for one nucleosome, as 50 nm corresponds to 150 bp.

Nucleosomes were also disrupted mechanically by increasing the tension, after supplementing B_0 with 50 mM NaCl and 2×10^{-3} % (w/v) nucleosome assembly protein-1 (NAP-1; gift from S. Leuba, University of Pittsburgh). At 7.7 pN, 14 individual lengthening steps with an average height of 24.2 ± 1.9 nm were detected (Fig. 2b), in agreement with ref. 6. Thanks to the presence of NAP-1, which interacts with core histones *in vitro*¹³ and favors their release, this process occurred at a lower force than in ref. 6. Notably, it was partially reversible, as also reported in ref. 6. In the course of two successive pulling phases at 7.7 pN, separated by a 50-s pause at

Figure 2 Micromanipulation of single chromatin fibers. (a) Extension-versus-rotation curves at 0.35 pN for an intact fiber (blue) in buffer B_0 (see Methods), for the same fiber after partial nucleosome disruption as shown in b (green) and for its corresponding naked DNA after complete nucleosome dissociation (red). (b) Individual nucleosome disruption events at 7.7 pN of the fiber in a in B_0 plus NAP-1 and 50 mM salt (see Results). The force was temporarily lowered to 0.67 pN between the arrows. (c) Maximal extension versus topological departure from DNA for ten fibers at 0.3 ± 0.07 pN in B_0 . Black straight line shows the relationship predicted by our three-state model (see Supplementary Discussion). Fibers on the line are referred to as regular and those off as irregular. Arrowheads correspond to the fibers studied in a (black) and d (blue). Numbers in green refer to fibers studied in Figure 6. (d) Extension-versus-rotation curves of the chromatin fiber corresponding to the blue arrowhead in c at 0.25 pN (blue) and of its corresponding renormalized DNA (red). Smooth curves were obtained assuming an elastic response in bending, stretching and twisting (worm-like rope model)¹⁵.

0.67 pN, the fiber contracted by -28.5 nm during the pause, roughly corresponding to one individual nucleosome reassociation.

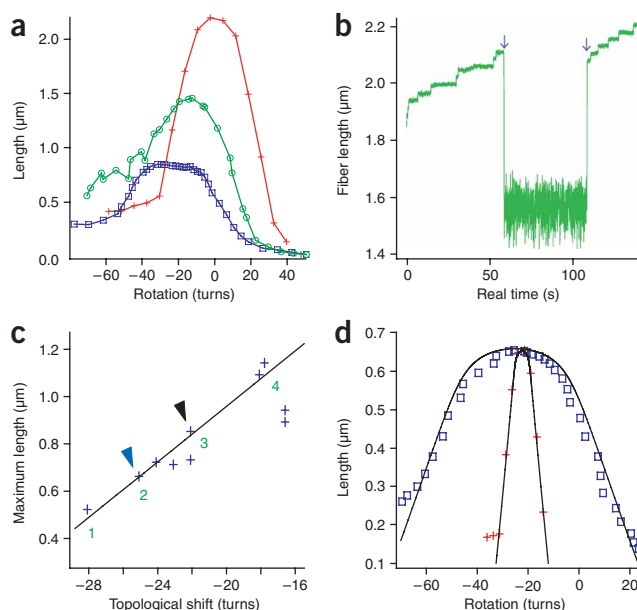
The response in torsion of the partially disrupted fiber was then probed in B_0 at low force and, as expected, it was intermediate between the responses of the original fiber and of DNA (Fig. 2a, green). The shifts in length and in topology between the new fiber and DNA were respectively ~ 700 nm and -13 ± 1.5 turns, or ~ 54 nm per turn, identical to the values derived for the initial fiber. Assuming that each step corresponds to the dissociation of one nucleosome, the topological deformation per nucleosome can be estimated as $-(11 \pm 1.5)/14 = -0.8 \pm 0.1$ turn.

The rotational behavior of ten fibers was then compared by plotting their maximal length at 0.3 ± 0.07 pN versus the rotational shift of those maxima relative to their corresponding naked DNAs (Fig. 2c). A linear trend was observed, with most data points well aligned and a slope close to 55 nm per turn. This is the expected behavior for regular nucleosome arrays with a variable number of nucleosomes. The corresponding nucleosome arrays were therefore referred to as regular. A few fibers, however, deviated from this linear trend. We show in the Supplementary Discussion online that these deviations can be attributed to the presence of variable proportions of clustered nucleosomes devoid of linker DNA (see also Supplementary Fig. 1 online). Hence, these fibers were termed irregular.

A direct comparison between chromatin and DNA requires a derivation of the torsional response of a DNA molecule having the same maximal length under the same force. Taking advantage of the invariance in length of the DNA torsional response⁸, one can obtain the renormalized curve of the DNA by dividing both lengths and rotations by the ratio of the maximal length of DNA to the maximal length of chromatin. The resulting renormalized DNA curve was further displaced parallel to the abscissa to superimpose its rotation center onto that of the fiber (Fig. 2d). Compared to DNA, nucleosome arrays seem extremely resilient, being able to accommodate a much larger amount of supercoiling without substantial shortening.

Stretching

The fiber described in Figure 2d and its corresponding DNA were also compared, again in B_0 , with respect to their stretching behaviors



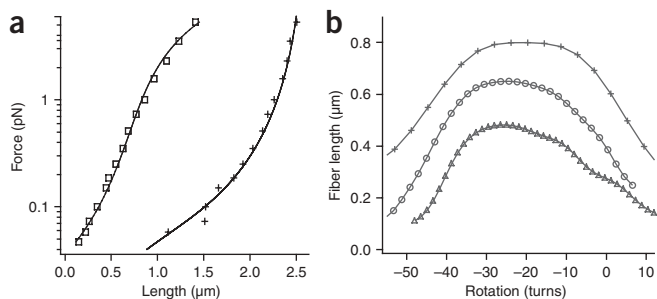


Figure 3 Tension dependence of the fiber behavior. (a) Force versus extension curves in B_0 of the fiber in **Figure 2c,d** (squares) and of the corresponding naked DNA (crosses) at their respective centers of rotation. Smooth curves were obtained as in **Figure 2d**. (b) Extension versus torsion of a regular fiber (same as charted in blue in **Fig. 2a**) in B_0 under tensions of 0.09 pN (triangles), 0.17 pN (circles) and 0.34 pN (crosses). Strong asymmetry in the mechanical response for positive compared to negative torsional constraints is observed at low forces. This is presumably a consequence of the different energies of the nucleosome's positive and negative states (see Results). The apex also shifts toward negative torsion at lower forces, presumably as a consequence of a shift in the equilibrium favoring nucleosomes in the negative conformation.

(**Fig. 3a**). Whereas chromatin is more rigid than DNA below 1 pN (the curve is steeper) in its entropic stretching regime (see below), beyond that force it becomes more flexible. This feature can be understood qualitatively as a consequence of the chromatin's three-dimensional arrangement: bending a wire in a spring-like shape can reduce its stretching modulus by orders of magnitude, a property extensively used in engineering.

The dependence of the rotational behavior on the applied force was also studied (**Fig. 3b**; with forces ranging from 0.09 pN to 0.34 pN). The torsional response always seemed more asymmetric at lower forces, and the curve's apex shifted toward negative values. This latter feature, which was not observed for naked DNA (not shown), indicates a larger topological deformation per nucleosome at lower force.

Salt effects

Several buffer conditions were investigated, and two of them, representative of the general trend, are documented here: B_0 plus 25 mM NaCl and B_0 plus 40 mM NaCl and 2 mM $MgCl_2$. Compared to the results with B_0 , the fibers always seemed more compact at higher salt concentrations (by $\sim 15\%$ in the first condition and $\sim 30\%$ in the second; **Fig. 4a** and **b**, respectively). Notably, the condensed fiber in salt could be extended to the length observed in B_0 by the transient application of a force of several pN. When the tension was released, the force-versus-length behavior became virtually identical to that obtained in B_0 . This property is consistent with the hysteresis loop observed in **Figure 4c**: the fiber was always longer upon decreasing the force than upon increasing it. A hysteresis was also observed in the rotational behavior: if a force of $\sim 2\text{--}3$ pN was exerted immediately before a torsional manipulation (typically performed at 0.3 pN), the response of the fiber was nearly identical to that previously recorded in B_0 at the same force (data not shown).

The reference behavior in B_0 therefore seems to correspond to a maximal extension of the fiber, in agreement with earlier observations that nucleosome arrays are decondensed in low salt¹⁴. The condensation and the hysteretic behavior in higher salt conditions presumably reflect short-range attractive nucleosome-nucleosome interactions mediated by histone tails, which can be temporarily broken by a transient force increase. These results are quite consistent with those reported in ref. 5, in which native chromatin was micromanipulated in tension under different salt conditions.

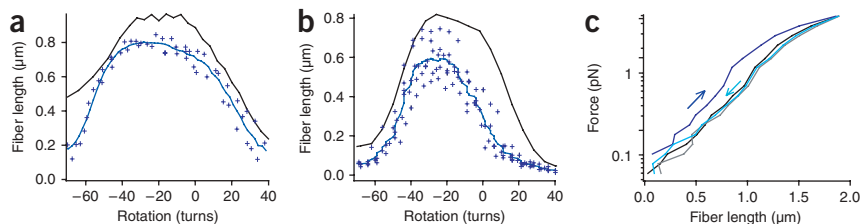
Despite a scattering intrinsic to the length measurements, a shift of the center of rotation toward more negative values was always observed in higher salt (**Fig. 4b**), as was also observed at lower force (**Fig. 3b**). For instance, the shift from B_0 to B_0 plus 40 mM NaCl and 2 mM $MgCl_2$ was -6 turns, that is ~ -0.25 turns per nucleosome (**Fig. 4b**).

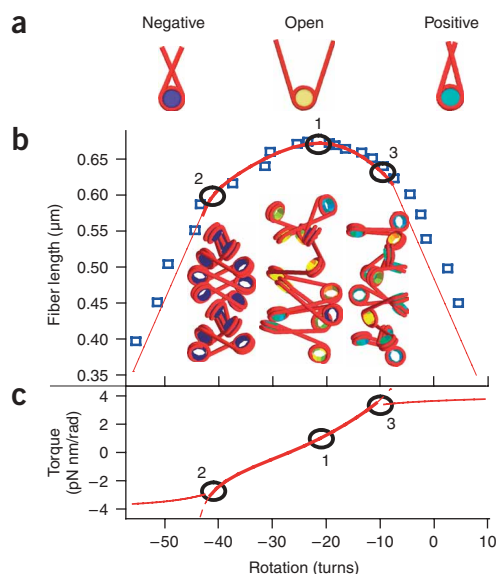
Worm-like rope modeling and canonical chromatin

The fiber's mechanical properties were first fitted using the worm-like rope model. This model, widely used for DNA¹⁵, represents a molecule (or, here, the chromatin fiber) as an isotropic elastic rod with defined bending, twisting and stretching moduli. This model fits well the length-versus-torsion and force-versus-length responses in **Figures 2** and **3**. The best-fit values of the bending persistence length and stretching modulus (28 nm and 8 pN, respectively) were in agreement with previous studies^{5,6} and models of the chromatin fiber^{16,17}. In contrast, the torsional persistence length, which was measured here for the first time, was exceptionally low (~ 5 nm, compared to ~ 80 nm for DNA).

As a first attempt to interpret this torsional resilience, we modeled two-angle nucleosomes^{18,19} with their entry/exit DNAs crossed negatively, as inferred from the core particle crystal structure² and observed with crystallized tetranucleosomes²⁰. Connecting these canonical nucleosomes by flexible DNA linkers led to the 'all-negative' fiber in

Figure 4 Salt-dependence of the fiber's mechanical behavior. (a) Extension-versus-rotation behavior of a fiber in B_0 (black) and in B_0 plus 25 mM NaCl (blue crosses; blue line shows filtered average) at 0.35 pN. (b) Extension-versus-rotation behavior of a fiber in B_0 (black) and in B_0 plus 40 mM NaCl and 2 mM $MgCl_2$ (blue crosses; blue line shows filtered average) at 0.2 pN. In high salt, an increased variability in the measurements is observed and the apex of the average curve shifts toward more negative rotation values, reflecting a displaced equilibrium with more nucleosomes in the negative state. (c) Response in force versus extension of the fiber in **a** at its center of rotation. In this experiment, we describe 'force cycles': first, the force on the fiber is increased step by step, and for each step the length of the fiber is recorded (dark blue and black). Once a constraint of ~ 5 pN is reached, the process is reversed, and the force is progressively lowered to its initial value (~ 0.05 pN; gray and cyan). The fiber does not show any hysteresis in B_0 (black and gray). In contrast, the fiber in B_0 plus 25 mM NaCl (dark blue and cyan) is initially more compact, but it can be extended to the B_0 level by a force of a few pN. Upon decrease in force, it behaves the same way as in low salt.





Supplementary Figure 2 online. Its very large torsional persistence length (35 nm, compared to 5 nm for the experimental value; see above) prompted us to turn to other concepts.

Mononucleosomes assembled on DNA minicircles

Previous studies have demonstrated that mononucleosomes thermally fluctuate between three discrete conformational states corresponding to different crossing statuses of entry/exit DNAs (with $\Delta L_{k_o} \sim -0.7$ (open, no crossing), $\Delta L_{k_n} \sim -1.4$ (closed negative, negative crossing) and $\Delta L_{k_p} \sim -0.4$ (closed positive, positive crossing) for the 5S positioning sequence (Fig. 5a)). The transition between these states involves a rotation of the nucleosome around its dyad relative to the loop^{10,21}. Notably, cryo-EM visualization of reconstituted fibers in low-salt conditions has also suggested the occurrence of such states²². In contrast, they do not appear in the tetranucleosome crystal structure²⁰, presumably because the high-salt conditions used for crystallization and the crystal packing energies favor closed conformations¹⁰.

The existence of the open state was first documented in minicircles²³, but it was only after the core particle crystal structure was disclosed² that the reason for such an easy unwrapping of the nucleosome edges became clear. DNA is attached to the octamer at 14 specific binding sites. These 14 sites are spaced every ~ 10 bp and are defined by their super-helix location (SHL) relative to the dyad². The SHL ± 6.5 sites are located at the nucleosome entry/exit and have the weakest binding energy²⁴. The existence of discrete open and closed states therefore results from the status of these sites, which can be only 'on' or 'off'.

The closed positive state shows a positive crossing of entry/exit DNAs. Although counterintuitive given the left-handed wrapping around the histone octamer, this state has been extensively documented using the minicircle approach through ethidium bromide fluorescence titration²⁵ and relaxation^{21,26,27}. We recently confirmed that SHL ± 6.5 binding sites are 'on' in this closed positive conformation. Indeed, the substitution of H3 Arg49 by a lysine, which, in contrast to arginine, cannot intercalate its basic lateral chain into the small groove of the DNA², equally affects the energies of the closed negative and closed positive states (N.C.e.S. & A.P., unpublished data).

Figure 5 Three-state model of the chromatin fiber. (a) Diagrams of individual nucleosomes in the negative ($\alpha \sim 54^\circ$; blue), open ($\alpha \sim -30^\circ$; yellow) and positive ($\alpha \sim 30^\circ$; cyan) states. (b) Torsional data (from same fiber as in Fig. 2d; squares) fitted by our three-state nucleosome model. The model fits the response over 30 turns around the apex (bold line). For higher torsion (on the positive and negative sides), a thin line representing the best fit using the pleconeme model is plotted. Under the curve are shown typical structures of a 208-bp repeat fiber at torsions marked by black circles (structures 1, 2 and 3). In structure 1, at the apex, 65%, 20% and 15% of nucleosomes, on average, are in the open, positive and negative conformations, respectively; in structure 2, the transition to the pleconeme regime on the negative side, 100% are negative, on average; in structure 3, the transition to the pleconeme regime on the positive side, 80% are positive and 20% are open, on average. (c) Torque as predicted by the three-state model (bold line) and by the pleconeme model (thin lines). Dashed line corresponds to the predicted evolution of the torque in the absence of pleconemes.

New model of the chromatin fiber

We constructed a new molecular model for the fiber (208-bp repeat length), assuming a thermodynamic equilibrium between the three different states of the nucleosome described above (Fig. 5a). A standard statistical mechanical analysis (free energy minimization based on the partition function) could then predict the fiber length-versus-torsion behavior at constant force, as a function of the energy differences between the states (see details in **Supplementary Discussion** and **Supplementary Equations 1–3** online). The upper part of the rotational response of a regular nucleosome array (corresponding to the blue arrowhead in Fig. 2c) was accurately fit by this model (Fig. 5b, bold line), using the number of nucleosomes (31) and the energy differences between the negative and open states ($U_n = +0.4$ kcal mol⁻¹, that is $+0.7 k_B T$ per molecule, where $k_B T$ is the thermal energy), and between the positive and open states ($U_p = +1.2$ kcal mol⁻¹, that is $+2 k_B T$) as adjustable parameters. The low energies involved imply that nucleosomes in the fiber are in a dynamic equilibrium and this equilibrium is displaced by the applied torsion. Three typical structures of fibers under specific rotational constraints are marked by black circles in Figure 5b. Structure 1 has the maximal extension and most of its nucleosomes in the open state. Structure 2 is

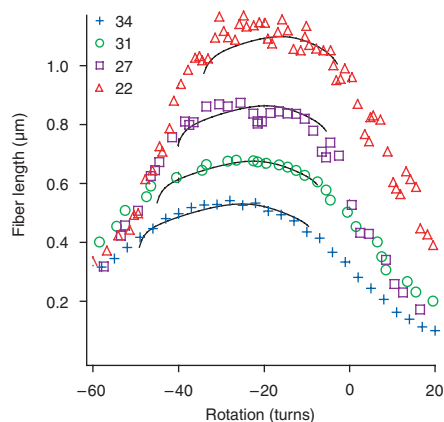


Figure 6 Single-parameter fitting. The torsional behavior of four regular fibers (corresponding to data labeled 1–4 in Fig. 2c) at 0.3 ± 0.07 pN in B_0 is plotted, together with their best fits using the three-state model. Each fit assumes a single set of energy differences for both the negative versus open state ($U_n = +0.4$ kcal mol⁻¹) and the positive versus open state ($U_p = +1.2$ kcal mol⁻¹) and adjusts the number of nucleosomes only; upper left key gives best-fit number of nucleosomes.

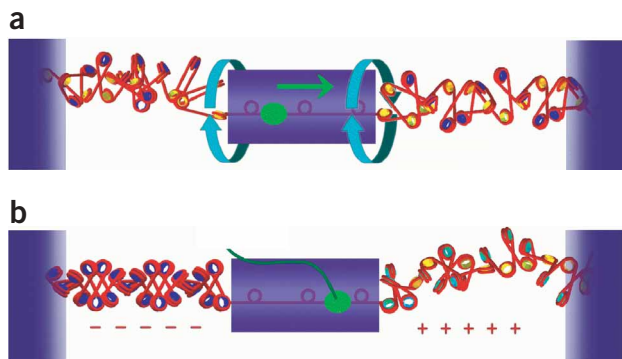


Figure 7 Chromatin as a topological buffer. Shown are schematics of the twin-supercoiled domain model of transcription³⁸ adapted to chromatin within the three-state model. Assuming that the fiber has clamped ends and that the transcription machinery cannot rotate around the helical axis of chromatin, the progression of the enzyme generates a positive torsional stress ahead of it (to the right) and a negative one in its wake (to the left). *In vivo*, proteins can ensure immobilization of the fiber ends, as in chromatin loops, for example. Blue box represents the transcription bubble, but does not denote any assumption regarding the fates of nucleosomes under transcription. (a) At the onset of transcription, the whole fiber is torsionally relaxed (Supplementary Fig. 4). Once started, the polymerase will keep moving until the increasing torques exerted by the left and right parts of the fiber balance the torque generated by the enzyme. (b) At the end of the elongation phase, the right part of the fiber is in a most-positive state (Fig. 5b, structure 3), whereas the left part is in an all-negative state (Fig. 5b, structure 2).

shorter, and essentially all of its nucleosomes are in the closed negative state. Structure 3 has an intermediate length and contains a mixture of open and closed positive nucleosomes (for comparison, 'all-open' and 'all-positive' fibers are shown in Supplementary Fig. 3 online; see also Supplementary Discussion).

The model also provides a prediction of the torque as a function of torsion (Fig. 5c; for a comparison with the curve obtained when considering the fiber as an isotropic elastic rod, see Supplementary Fig. 4 online). The torque is less than 3 pN nm rad^{-1} over ~ 30 turns around the center of rotation, that is, substantially smaller than that exerted by polymerases ($>5 \text{ pN nm rad}^{-1}$)²⁸ or than the value predicted for nucleosome torsional ejection (9 pN nm rad^{-1})²⁹.

Notably, the behavior of all regular nucleosome arrays can be described with the same set of energy values by fitting the number of nucleosomes only (Fig. 6). The fitted energies ($U_n = +0.4 \text{ kcal mol}^{-1}$ and $U_p = +1.2 \text{ kcal mol}^{-1}$; see above) are close to those obtained in the minicircle system under conditions of maximal repulsion of entry/exit DNAs ($U_n = +0.5 \text{ kcal mol}^{-1}$ and $U_p = +2.2 \text{ kcal mol}^{-1}$ (ref. 10)). Considering the differences in geometry and ionic environment between the two systems, our best-fit values seem to be fully consistent with minicircle data.

Response to high torsional stress

Once ~ -20 turns have been applied starting from the apex, the model predicts that all nucleosomes should be in the closed negative state (Fig. 5b, structure 2). Because the fiber in the model cannot accommodate more negative turns by nucleosome transitions, the torque then increases abruptly (Fig. 5c, dotted line). In the experimental curve, a marked change in the length-versus-rotation curve is indeed observed beyond ~ -20 turns, associated with a constant slope of $\sim -25 \text{ nm per turn}$. By analogy with naked DNA⁸, we interpret this constant slope as a consequence of plectoneme formation. Notably, 25 nm per turn is much smaller than the 90 nm per turn obtained for naked DNA at the same force, which indicates a lower torque (3 pN nm rad^{-1} for chromatin compared to 6 pN nm rad^{-1} for naked DNA; see Supplementary Discussion). Hence, plectonemes cannot form in the DNA spacers flanking the nucleosome array (Fig. 1); they must form in the fiber itself. Indeed, plectoneme formation may be facilitated in chromatin for two reasons. First, the energy cost of bending is a major component of the free energy of formation of plectonemes on naked DNA. This cost should be reduced by nucleosomes, which are natural DNA benders. (The bending persistence length of the fiber is indeed smaller than that of DNA; see above.) Second, the DNA charge screening of entry/exit DNAs through interactions with H3 N-terminal tails^{30,31} may also contribute to reduction of electrostatic repulsion and thus may favor compact

'twisted-pairs' conformations that occur in plectonemes. This process is expected to extrude nucleosomes away from the plectoneme axis (Supplementary Fig. 5 online).

Plectonemes should also develop on the positive side of the rotation curve, and indeed, a transition to a linear slope of $\sim 25 \text{ nm per turn}$ occurs at $\sim +10$ turns from the apex. This corresponds to a supercoiling substantially lower than on the negative side. Our model, however, predicts that the corresponding torque should still be $\sim 3 \text{ pN nm rad}^{-1}$ (see Supplementary Discussion), a value similar to that obtained on the negative side. This discrepancy between the negative and the positive behavior is a direct consequence of the higher energy of the positive state as compared to the negative one. Our model consistently indicates that only a fraction of the nucleosomes are in the closed positive state at the onset of plectoneme formation (Fig. 5b, structure 3); the torque necessary to drive the fiber into an all-positive conformation is higher than the critical torque for plectoneme formation.

DISCUSSION

Nucleosome transitions and chromatin topology

These nanomanipulation experiments show that regular chromatin fibers are torsionally resilient structures that can accommodate large positive and negative supercoiling without developing strong torques or undergoing much shortening. We interpreted this resilience, typically five times higher than that predicted for a canonical fiber of closed negative nucleosomes, as being the consequence of a dynamic equilibrium occurring between three conformational states of the nucleosome. A molecular model based on this equilibrium quantitatively accounts for the data and delineates the energy landscape involved in the nucleosome transitions.

This dynamic nature of chromatin provides simple explanations to several long-standing puzzles about the topology of DNA in chromatin. The most well known is the so-called 'linking-number paradox': why does a 2-turn particle reduce the DNA linking number by 1 instead of 2 (refs. 10,32,33)? At first, the DNA was proposed to become overtwisted upon wrapping on the histone surface³², but it was later recognized that, even if some overtwisting may occur, it is by no means sufficient to explain the discrepancy⁴. The true explanation may, therefore, lie in a dynamic topological compensation occurring between negatively and positively crossed nucleosomes.

Several other pending questions find simple answers thanks to our results. (i) The shift of the ΔLk per nucleosome observed for a minichromosome reconstituted on the same 5S repeats as used here, from -1.0 with control histones to -0.8 with hyperacetylated histones (that is, under high mutual repulsion of linker DNAs)³⁴ is due to a displacement of the dynamic equilibrium toward more nucleosomes

in the open state. The same occurred in our experiment (Fig. 4b): $\Delta Lk \sim -1$ was obtained in higher salt, compared to $\Delta Lk \sim -0.8$ in B_0 (also favoring entry/exit DNA repulsion). Notably, a similar $\sim +0.2$ shift in ΔLk was also measured in the minicircle system with acetylated mononucleosomes in phosphate, a buffer that further destabilizes interactions between histone tails and DNA¹⁰. (ii) Reconstituted minichromosomes can withstand as much negative supercoiling ($\sigma \sim -0.1$) as the corresponding naked DNA upon treatment with DNA gyrase³⁵. The nucleosome's apparent 'transparency' to that enzyme in spite of the trapping of most DNA in the nucleosome cores can be explained by a shift of most nucleosomes to the negative state¹⁰ rather than by a forced undertwisting of the DNA on the histone surface³⁴. (iii) Finally, the ability of positively supercoiled plasmids to withstand the reconstitution of a large number of nucleosomes, in spite of the large additional positive supercoiling expected to accumulate³⁶, must similarly reflect the displacement of nucleosomes toward the positive state.

Chromatin as a topological buffer

One may question the biological relevance of conclusions about the topology of nucleosomes drawn from experiments performed on chromatin fibers devoid of linker histones (such as H1). Linker histones cannot bind nucleosomes in the open state, but they do bind nucleosomes in the negative and positive states, and this brings entry/exit DNAs together into a torsionally highly flexible stem²⁷. Also, the binding energy of linker histones on the nucleosomes is rather low, considering the dynamics of these proteins in live cells^{11,12,37}. The presence of linker histones may thus alter substantially the equilibrium between the three states and in particular decrease the proportion of the open state. However, this should not suppress the high resilience still associated with the equilibrium between the closed negative and the closed positive states. Consequently, even if the steady-state proportion of open-state nucleosomes is small in quiescent chromatin, H1-containing fibers with nucleosomes in the closed negative and closed positive states should remain highly resilient. Open nucleosomes may rather be more involved in active chromatin, as suggested by two observations. First, histone acetylation, which favors the open state (see above), is usually associated with transcription. Second, H2A–H2B dimers are much more easily removed by NAP-1 when nucleosomes are in the open state than in the negative state, and their removal results in further unwrapping and the formation of single-turn tetrasomes (N.C.e.S. & A.P., unpublished data).

Chromatin torsional resilience must have important *in vivo* implications, because DNA transactions usually involve topological changes. Consider, for instance, the twin–supercoiled domain model of transcription³⁸ in the context of chromatin. Our three-state model predicts that a fiber containing 50 nucleosomes and clamped at both ends can accommodate the supercoiling generated by the transcription of about 100 bp without the help of topoisomerases and without exceeding the torque exerted by the polymerase (Fig. 7), thus acting as a powerful 'topological buffer.' The transcription of 100 bp would indeed induce ~ 10 positive turns on the right part of the fiber and ~ 10 negative turns on the left side. The Lk difference between a relaxed and an 'all-negative' or a 'most-positive' fiber is ~ -0.5 or $\sim +0.4$ per nucleosome, respectively (see Fig. 5b and Supplementary Fig. 4). For these two constrained states of the fiber, the torque is ~ 3 pN nm rad⁻¹. Hence, the total torque is ~ 6 pN nm rad⁻¹, close to the torque exerted by the polymerase, at least 5 pN nm rad⁻¹ (ref. 28). We conclude that a fiber containing ~ 50 nucleosomes (equivalent to a topological buffer of $\sim 25 \times 0.4 = 10$ turns) can sustain

the transcription of 100 bp with no need for relaxation by a topoisomerase. The chromatin's capacity to accommodate torsion should therefore favor the smooth progression of tracking enzymes and protect nucleosomes from unsolicited destruction by positive supercoiling. Notably, the polymerase's torque seems to lie just below the combined thresholds for plectoneme formation on the upstream and downstream parts of the fiber, that is, below the torque at which the fiber should begin to dramatically shorten and change its large-scale organization. Whether this is a mere coincidence or a biologically relevant feature (for example, preventing the action of polymerases from dramatically altering chromatin organization if the torque is not relaxed efficiently enough) will deserve further investigation.

Nucleosome conformational transitions may also have a role in the control of DNA-protein interactions in the context of chromatin, for instance by affecting the binding of linker histones and their HMG protein competitors³⁹. In addition, they may affect the binding of other proteins, such as remodeling or transcription factors¹², in a torsion-dependent manner, by means of rearrangements in the fiber's three-dimensional architecture (as in Figs. 5 and 7, for example).

As suggested in ref. 39, dynamic binding of proteins on chromatin^{11,12,37} offers an efficient way to quickly react to changes in the environment. Because they depend on the fiber torsion, the transitions revealed and discussed in the present work may provide the conditions for coupling between this dynamic binding and the action of tracking enzymes. Such coupling has the notable property of being both long-range and much faster than any molecular transport process. It is thus a particularly interesting candidate for quickly responding regulatory mechanisms.

METHODS

Nucleosome arrays preparation. Nucleosome arrays were reconstituted by conventional stepwise dilution. The nucleosome density was checked by sedimentation in sucrose gradients⁴⁰ and the nucleosome array's regularity probed by micrococcal nuclease digestion (data not shown).

Three DNA fragments were prepared by PCR: two were amplified from the linearized template Litmus28i (NEB, positions 2008 and 2580) with modified biotin or digoxigenin nucleotides (Roche); the third was obtained by amplifying the pFOS-1 template (NEB, positions 3803 and 4539) with standard nucleotides. Appropriate restriction digestions of the PCR products led to 554- and 620-bp fragments. These fragments were ligated into two different 1,174-bp 'hybrids,' consisting of one part (620 bp) unmodified DNA and another part (574 bp) DNA modified with biotin or digoxigenin.

The two hybrid fragments were then ligated to the nucleosome arrays to give the final construction (Fig. 1). The fibers were finally dialyzed against TE buffer (10 mM Tris-HCl (pH 7.5) and 1 mM EDTA) and stored at -20°C after a two-fold dilution with 100% (v/v) glycerol.

Magnetic tweezers apparatus. A poly-di-methylsiloxane (PDMS; Dow-Corning) flow cell with a 2-mm-wide and 80- μm -high channel was constructed. This microfluidic cell was mounted on a glass coverslip treated with 3-mercaptopropyl-trimethoxysilane (Sigma)⁴¹. The surface-coating was performed inside the channel with nonspecific binding of anti-digoxigenin (Roche) for 1 h at 37°C , followed by overnight BSA blocking.

The PDMS flow cell was placed beneath two NdFeB permanent magnets (HPMG) separated by 0.8 mm⁴¹. Images were grabbed by a CCD camera (JAI). From the transverse fluctuations magnitude and the molecule length, the exact force acting on the bead was deduced⁸. Moving the magnets up and down by ~ 5 mm permits a range of forces from 0.1 pN to 15 pN. The topological constraint was controlled by rotation of the magnets about the vertical axis.

Nucleosome array injection and study. Just before the experiment, 1 ng of chromatin, previously diluted to 10 μl with TE, was mixed with 100 μg of 2.8- μm -diameter streptavidin-coated magnetic beads (Dyna). After 1 min of

incubation, the solution was aspirated into the cell by a syringe pump. Data were usually acquired in TE plus 0.01% (w/v) BSA (buffer B₀). The standard buffer was B₀ because, at this low ionic strength, nucleosomes are very stable and do not move along DNA⁴², and nucleosome-nucleosome interactions are weak⁴³.

Chemical nucleosome disruption. At the end of each experiment, nucleosomes were chemically disassembled by aspirating into the flow cell a solution containing 0.01% (w/v) heparin (Dakota Pharm) in B₀ for 10 min.

Note: Supplementary information is available on the Nature Structural & Molecular Biology website.

ACKNOWLEDGMENTS

The authors are grateful to G. Almouzni and J.P. Quivy for providing material in preliminary experiments, E. Ben-Haim and C. Bouchiat for discussions and K. Dorfman and A. Sivolob for critical reading. A.B., N.C.e.S., G.W., C.L. and J.M. thank the French Ministry of Research for AC-MENRT fellowships. This work was supported by the Centre National de la Recherche Scientifique (A.P.'s and J.M.V.'s laboratories) and by grants from the Centre National de la Recherche Scientifique/Ministère de l'Éducation Nationale de la Recherche et de la Technologie DRAB programs and the Institut Curie Physics of the Cell cooperative program (J.L.V.'s laboratory).

COMPETING INTERESTS STATEMENT

The authors declare that they have no competing financial interests.

Published online at <http://www.nature.com/nsmb>

Reprints and permissions information is available online at <http://npg.nature.com/reprintsandpermissions/>

1. VanHolde, K.E. *Chromatin* (Springer-Verlag, New York, 1988).
2. Luger, K., Mader, A.W., Richmond, R.K., Sargent, D.F. & Richmond, T.J. Crystal structure of the nucleosome core particle at 2.8 Å resolution. *Nature* **389**, 251–260 (1997).
3. Germond, J.E., Hirt, B., Oudet, P., Gross-Bellard, M. & Chambon, P. Folding of the DNA double helix in chromatin-like structures from simian virus 40. *Proc. Natl. Acad. Sci. USA* **72**, 1843–1847 (1975).
4. Wolffe, A. *Chromatin* (Academic Press, London, 1998).
5. Cui, Y. & Bustamante, C. Pulling a single chromatin fiber reveals the forces that maintain its higher-order structure. *Proc. Natl. Acad. Sci. USA* **97**, 127–132 (2000).
6. Brower-Toland, B.D. *et al.* Mechanical disruption of individual nucleosomes reveals a reversible multistage release of DNA. *Proc. Natl. Acad. Sci. USA* **99**, 1960–1965 (2002).
7. Hayes, J.J. & Hansen, J.C. New insights into unwrapping DNA from the nucleosome from a single-molecule optical tweezers method. *Proc. Natl. Acad. Sci. USA* **99**, 1752–1754 (2002).
8. Strick, T.R., Allemand, J.F., Bensimon, D., Bensimon, A. & Croquette, V. The elasticity of a single supercoiled DNA molecule. *Science* **271**, 1835–1837 (1996).
9. Simpson, R.T., Thoma, F. & Brubaker, J.M. Chromatin reconstituted from tandemly repeated cloned DNA fragments and core histones: a model system for study of higher order structure. *Cell* **42**, 799–808 (1985).
10. Prunell, A. & Sivolob, A. Paradox lost: nucleosome structure and dynamics by the DNA minicircle approach. in *Chromatin Structure and Dynamics: State-of-the-Art* Vol. 39 (eds. Zlatanova, J. & Leuba, S.H.) 45–73 (Elsevier, London, 2004).
11. Catez, F. *et al.* Network of dynamic interactions between histone H1 and high-mobility-group proteins in chromatin. *Mol. Cell. Biol.* **24**, 4321–4328 (2004).
12. Phair, R.D. *et al.* Global nature of dynamic protein-chromatin interactions *in vivo*: three-dimensional genome scanning and dynamic interaction networks of chromatin proteins. *Mol. Cell. Biol.* **24**, 6393–6402 (2004).
13. McBryant, S.J. *et al.* Preferential binding of the histone (H3–H4)₂ tetramer by NAP1 is mediated by the amino-terminal histone tails. *J. Biol. Chem.* **278**, 44574–44583 (2003).
14. Leuba, S.H. *et al.* Three-dimensional structure of extended chromatin fibers as revealed by tapping-mode scanning force microscopy. *Proc. Natl. Acad. Sci. USA* **91**, 11621–11625 (1994).
15. Bouchiat, C. & Mezard, M. Elasticity model of a supercoiled DNA molecule. *Phys. Rev. Lett.* **80**, 1556–1559 (1998).
16. Ben-Haim, E., Lesne, A. & Victor, J.M. Chromatin: a tunable spring at work inside chromosomes. *Phys. Rev. E Stat. Nonlin. Soft Matter Phys.* **64**, 051921 (2001).
17. Schiessel, H., Gelbart, W.M. & Bruinsma, R. DNA folding: structural and mechanical properties of the two-angle model for chromatin. *Biophys. J.* **80**, 1940–1956 (2001).
18. Woodcock, C.L., Grigoriev, S.A., Horowitz, R.A. & Whitaker, N. A chromatin folding model that incorporates linker variability generates fibers resembling native structures. *Proc. Natl. Acad. Sci. USA* **90**, 9021–9025 (1993).
19. Barbi, M., Mozziconacci, J. & Victor, J.M. How the chromatin fiber deals with topological constraints? *Phys. Rev. E Stat. Nonlin. Soft Matter Phys.* **71**, 031910 (2005).
20. Schalch, T., Duda, S., Sargent, D.F. & Richmond, T.J. X-ray structure of a tetra-nucleosome and its implications for the chromatin fiber. *Nature* **436**, 138–141 (2005).
21. De Lucia, F., Alilat, M., Sivolob, A. & Prunell, A. Nucleosome dynamics. III. Histone tail-dependent fluctuation of nucleosomes between open and closed DNA conformations. Implications for chromatin dynamics and the linking number paradox. A relaxation study of mononucleosomes on DNA minicircles. *J. Mol. Biol.* **285**, 1101–1119 (1999).
22. Bednar, J. *et al.* Nucleosomes, linker DNA, and linker histone form a unique structural motif that directs the higher order folding and compaction of chromatin. *Proc. Natl. Acad. Sci. USA* **95**, 14173–14178 (1998).
23. Goulet, I., Zivanovic, Y., Prunell, A. & Revet, B. Chromatin reconstitution on small DNA rings. I. *J. Mol. Biol.* **200**, 253–266 (1988).
24. Luger, K. & Richmond, T.J. DNA binding within the nucleosome core. *Curr. Opin. Struct. Biol.* **8**, 33–40 (1998).
25. Sivolob, A., De Lucia, F., Revet, B. & Prunell, A. Nucleosome dynamics. II. High flexibility of nucleosome entering and exiting DNAs to positive crossing. An ethidium bromide fluorescence study of mononucleosomes on DNA minicircles. *J. Mol. Biol.* **285**, 1081–1099 (1999).
26. Sivolob, A., Lavelle, C. & Prunell, A. Sequence-dependent nucleosome structural and dynamic polymorphism. Potential involvement of histone H2B N-terminal tail proximal domain. *J. Mol. Biol.* **326**, 49–63 (2003).
27. Sivolob, A. & Prunell, A. Linker histone-dependent organization and dynamics of nucleosome entry/exit DNAs. *J. Mol. Biol.* **331**, 1025–1040 (2003).
28. Harada, Y. *et al.* Direct observation of DNA rotation during transcription by *Escherichia coli* RNA polymerase. *Nature* **409**, 113–115 (2001).
29. Sarkar, A. & Marko, J.F. Removal of DNA-bound proteins by DNA twisting. *Phys. Rev. E Stat. Nonlin. Soft Matter Phys.* **64**, 061909 (2001).
30. Shaw, S.Y. & Wang, J.C. Knotting of a DNA chain during ring closure. *Science* **260**, 533–536 (1993).
31. Angelov, D., Vitolo, J.M., Mutskov, V., Dimitrov, S. & Hayes, J.J. Preferential inter-reaction of the core histone tail domains with linker DNA. *Proc. Natl. Acad. Sci. USA* **98**, 6599–6604 (2001).
32. Klug, A. & Lutter, L.C. The helical periodicity of DNA on the nucleosome. *Nucleic Acids Res.* **9**, 4267–4283 (1981).
33. Prunell, A. A topological approach to nucleosome structure and dynamics: the linking number paradox and other issues. *Biophys. J.* **74**, 2531–2544 (1998).
34. Norton, V.G., Imai, B.S., Yau, P. & Bradbury, E.M. Histone acetylation reduces nucleosome core particle linking number change. *Cell* **57**, 449–457 (1989).
35. Garner, M.M., Felsenfeld, G., O'Dea, M.H. & Gellert, M. Effects of DNA supercoiling on the topological properties of nucleosomes. *Proc. Natl. Acad. Sci. USA* **84**, 2620–2623 (1987).
36. Clark, D.J., Ghirlando, R., Felsenfeld, G. & Eisenberg, H. Effect of positive supercoiling on DNA compaction by nucleosome cores. *J. Mol. Biol.* **234**, 297–301 (1993).
37. Misteli, T., Gunjan, A., Hock, R., Bustin, M. & Brown, D.T. Dynamic binding of histone H1 to chromatin in live cells. *Nature* **408**, 877–881 (2000).
38. Liu, L.F. & Wang, J.C. Supercoiling of the DNA template during transcription. *Proc. Natl. Acad. Sci. USA* **84**, 7024–7027 (1987).
39. Bustin, M., Catez, F. & Lim, J.H. The dynamics of histone H1 function in chromatin. *Mol. Cell* **17**, 617–620 (2005).
40. Hansen, J.C. & Lohr, D. Assembly and structural properties of subsaturated chromatin arrays. *J. Biol. Chem.* **268**, 5840–5848 (1993).
41. Fulconis, R. *et al.* Twisting and untwisting a single DNA molecule covered by RecA protein. *Biophys. J.* **87**, 2552–2563 (2004).
42. Meersseman, G., Pennings, S. & Bradbury, E.M. Mobile nucleosomes—a general behavior. *EMBO J.* **11**, 2951–2959 (1992).
43. Mangenot, S., Leforestier, A., Durand, D. & Livolant, F. X-ray diffraction characterization of the dense phases formed by nucleosome core particles. *Biophys. J.* **84**, 2570–2584 (2003).